World Scientific News

A new approach to porous PEO coating sub-layers determination on the basis of GDOES signals

Krzysztof Rokosz[1,a]**, Tadeusz Hryniewicz**[1,b]**, Patrick Chapon**[2,c]**, Łukasz Dudek**[1,d]

[1]Division of Bioengineering and Surface Electrochemistry, Department of Engineering and Informatics Systems, Koszalin University of Technology, 15-17 Racławicka Str., PL 75-620 Koszalin, Poland

[2] HORIBA Jobin Yvon S.A.S., 16-18, rue du Canal - 91165 Longjumeau Cedex, France

[a-d]E-mail address: rokosz@tu.koszalin.pl , Tadeusz.Hryniewicz@tu.koszalin.pl , patrick.chapon@horiba.com , lukasz.dudek@tu.koszalin.pl

ABSTRACT

In present work, an approach to porous PEO coating sub-layers determination on the basis of Glow-Discharge Optical Emission Spectroscopy (GDOES) measurements, is presented. CP Titanium Grade 2 was used for the study. By interpreting the depth profiles obtained by GDOES, the Authors could reveal boundaries of zones with specific features in the obtained coating. This way the porous PEO coating can be divided into different sub-layers. The use of the first and second derivatives of hydrogen, phosphorus and titanium signals in the GD profiles allowed to determine these sub-layers, with results shown in that article.

Keywords: model of PEO coating; Plasma Electrolytic Oxidation (PEO); Micro Arc Oxidation (MAO); CP Titanium Grade 2; Glow-Discharge Optical Emission Spectroscopy (GDOES); porous coating

1. INTRODUCTION

Production of porous coatings on biomaterials is very important due to the assimilation of the implants to the living organisms. In case of nanolayers with most likely pico-porosity, which may be obtained by electropolishing EP [**1-5**], magnetoelectropolishing MEP [**5-16**] or

high-current density electropolishing HDEP [**17-19**] the most important parameter is the chemical composition of passive layers obtained. In addition, it has to be pointed out that by using those electrochemical methods it is possible to enrich those nanolayers in different chemical elements in order to increase their corrosion resistance as well as decrease the amount of elements which can sensitize, *i.e.* nickel, aluminum, or chromium on the sixth oxidation stage.

On the other hand for porous microlayers, which can be also enriched in selected chemical elements, such as antimicrobial copper [**20-25**], the entire porous zone is interacting with the environment. Such porous layers may be formed with the use of Plasma Electrolytic Oxidation (PEO) known also as Micro Arc Oxidation (MAO) [**26-35**]. To understand the formation process of PEO coatings it is necessary to find out and propose an approach to describe these sub-layers of PEO coatings and we have used for that Glow-Discharge Optical Emission Spectroscopy (GDOES) signals [**36-37**]. The paper aims at describing this novel original method.

2. METHOD

The samples of CP Titanium Grade 2 after Plasma Electrolytic Oxidation (Micro Arc Oxidation) were treated for the surface studies. At the beginning, the samples were polished by mechanical treatment in the form of rectangular specimens of dimensions 30×10 mm cut off from the metal sheet 2 mm thick. The plasma electrolytic oxidation (PEO) was performed at the voltage of 450 ±10 V. The studies were carried out in the electrolyte of initial temperature of 20 ±2 °C. For the studies, the electrolyte based on orthophosphoric acid H_3PO_4 with copper nitrate $Cu(NO_3)_2$, was used. For each run, the electrolytic cell made of glass was used, containing up to 500 ml of the electrolyte. GDOES sputters a representative area of the sample of interest (in our case 4 mm in diameter), the sputtered species being simultaneously excited by the GD plasma. The observed signals therefore represent at each time an average of the sputtered area. Measurements were done with a Horiba Scientific GD Profiler 2 instrument using RF asynchronous pulse generator under the plasma conditions (pressure: 700 Pa, power: 40 W, frequency: 3000 Hz, duty cycle: 0.25, anode diameter: 4 mm). The signals of copper (325 nm), phosphorus (178 nm), oxygen (130 nm), hydrogen (122 nm), and titanium (365 nm), were measured.

3. RESULTS AND DISCUSSION

In **Figures 1-5**, the GDOES depth profiles signals of titanium, phosphorus, copper, oxygen and hydrogen with their first and second derivatives are presented. Due to the roughness of the materials, the original signals feature slow changing trends making difficult the finding of the sub-layers of the PEO coating and so, the Authors decided to use the first and second derivatives, which may better reveal the boundaries of these sub-layers.

Based on titanium, phosphorus, oxygen and copper signals, it is possible to state that the PEO coating is found up to a depth corresponding to a sputtering time of about 900 s. All the spectra show a top surface zone with high amount of contamination from the start until about 50 s of sputtering time.
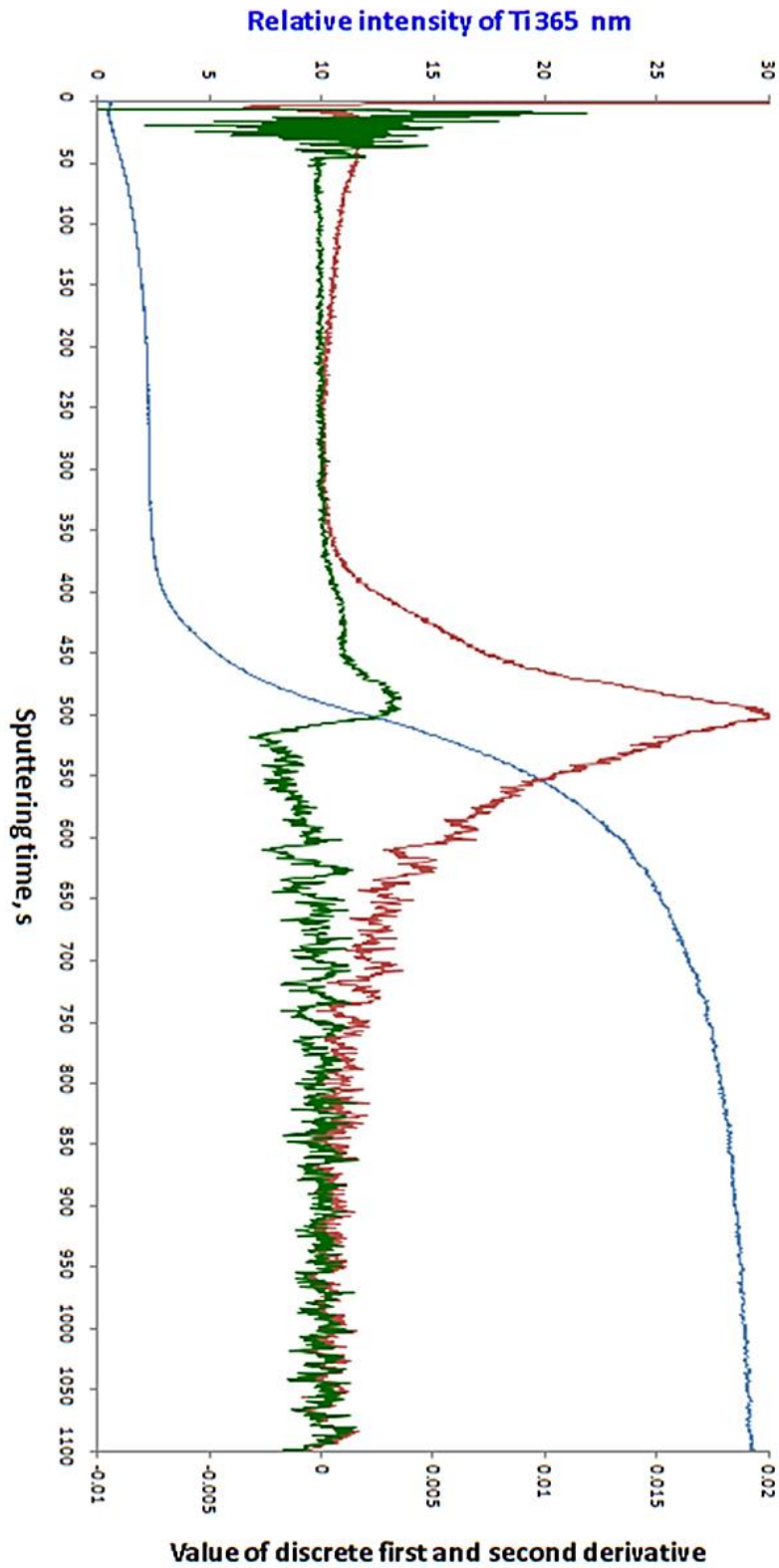
Fig. 1. GDOES results of titanium signal (blue line) and its first and second derivatives by sputtering time (corresponding brown and red lines) of PEO coating formed on titanium
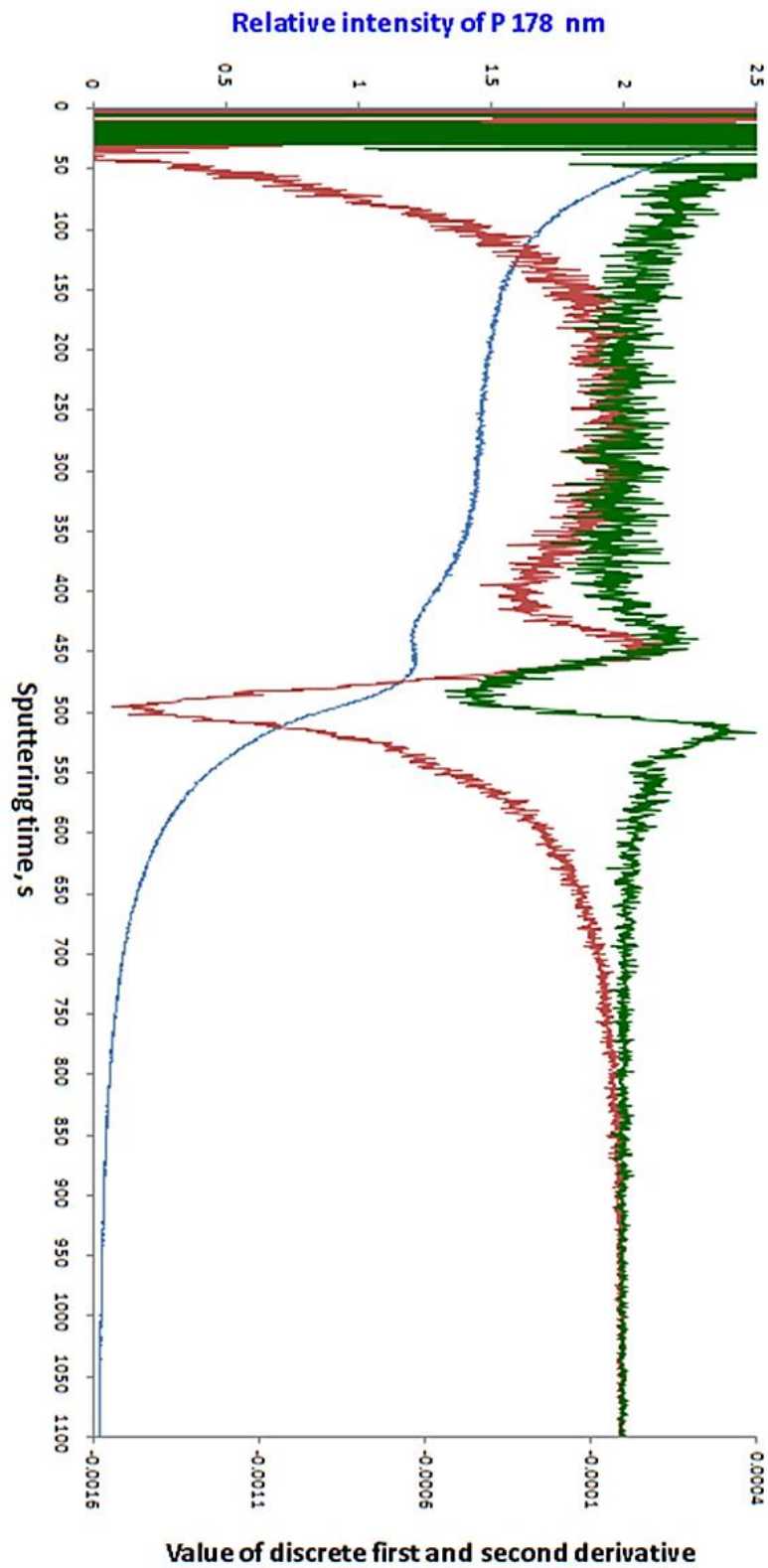
Fig. 2. GDOES results of phosphorus signal (blue line) and its first and second derivatives by sputtering time (corresponding brown and red lines) of PEO coating formed on titanium
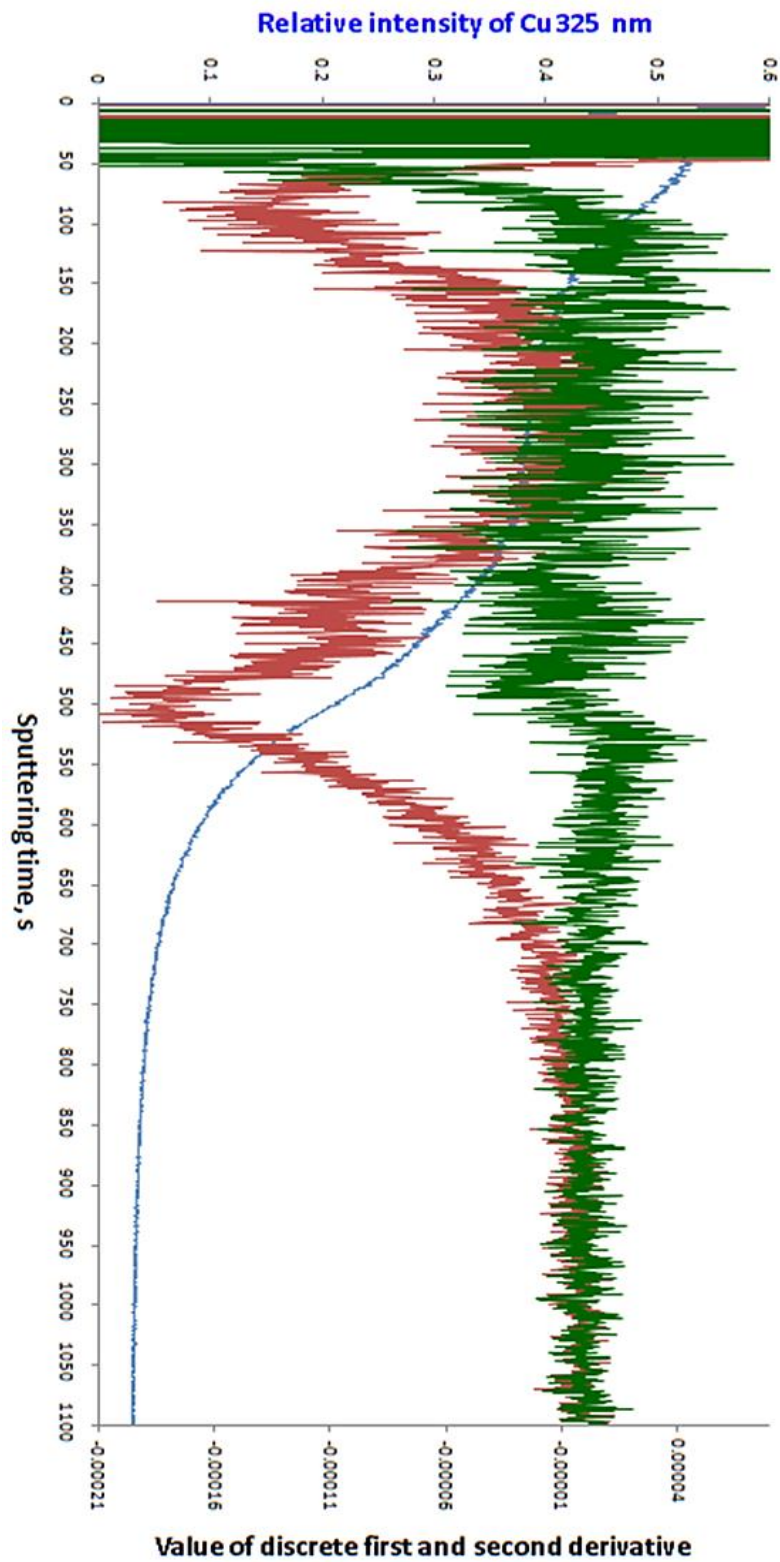
Fig. 3. GDOES results of copper signal (blue line) and its first and second derivatives by sputtering time (corresponding brown and red lines) of PEO coating formed on titanium

Fig. 4. GDOES results of oxygen signal (blue line) and its first and second derivatives by sputtering time (corresponding brown and red lines) of PEO coating formed on titanium

Fig. 5. GDOES results of hydrogen signal (blue line) and its first and second derivatives by sputtering time (corresponding brown and red lines) of PEO coating formed on titanium.
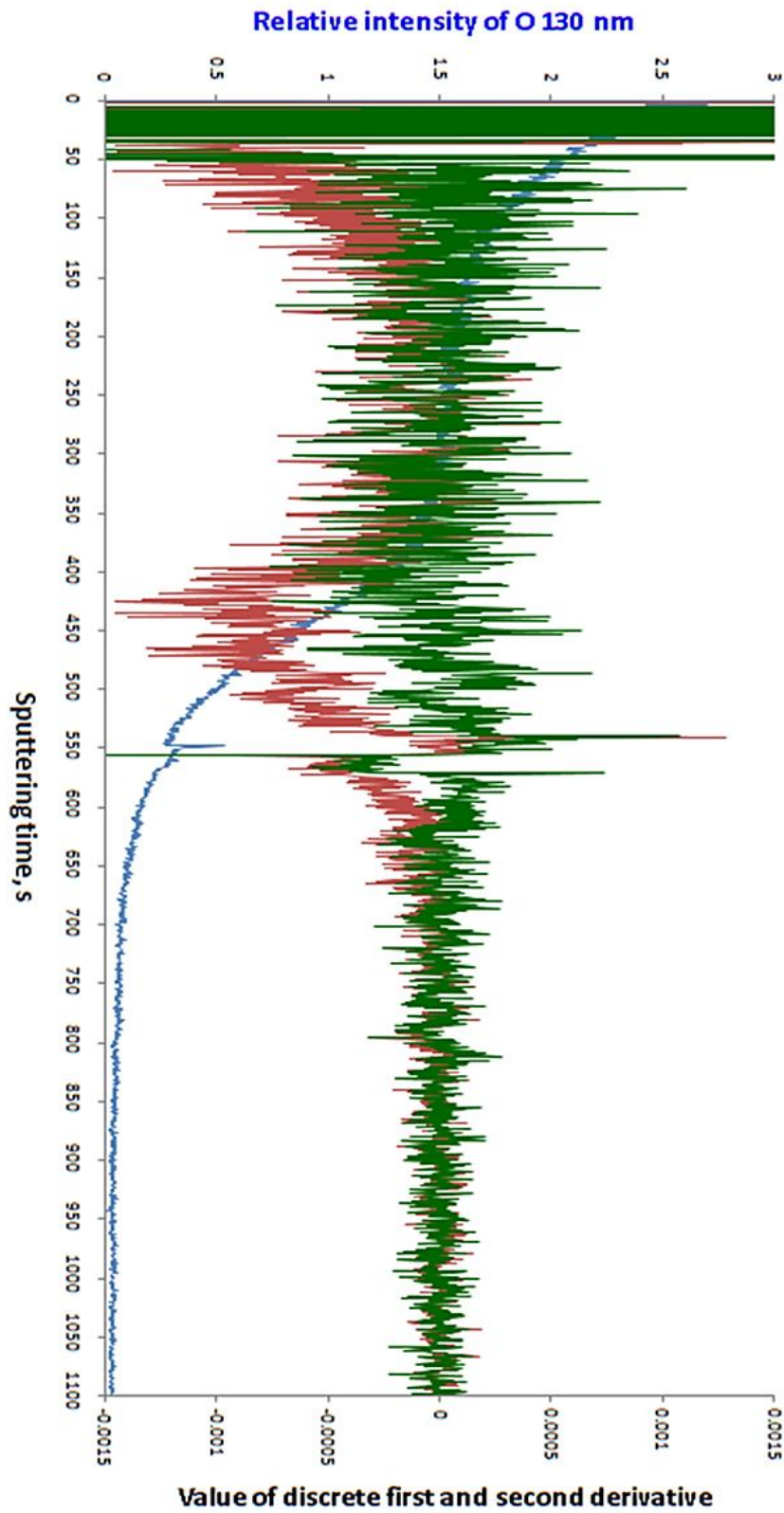
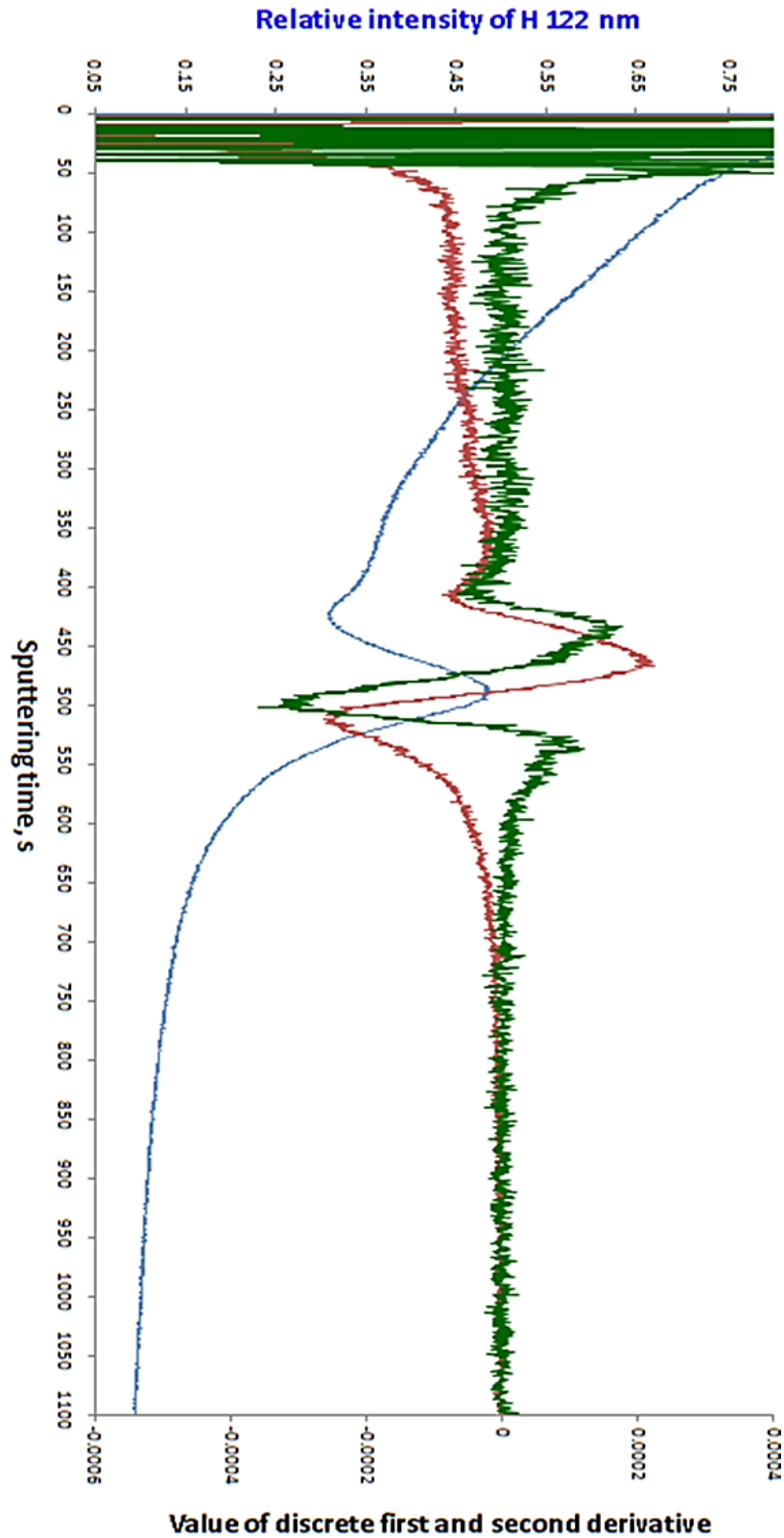The next sub-layer is located at the depth corresponding to sputtering time from 50 s up to about 350 s. That sub-layer is enriched in copper, phosphorous and oxygen. The following sub-layer, the transition one, is located under the previous layer, *i.e.* at a depth corresponding to sputtering time in the range of 350 s to 900 s.

Authors decided that the penetration of organic contamination (revealed by C and H signals) inside the PEO coating most likely is the tracer of the boundary of the presence of porosity. Therefore on the basis of the hydrogen signal and its first and second derivatives (Fig. 5), it is possible to find the boundary of that porosity, which is at a depth corresponding up to about 750 s of sputtering time.

4. CONCLUSIONS

The investigation carried out GDOES measurements on CP Titanium Grade 2 after PEO processing allowed to formulate the following conclusions:

- the first and second derivatives of GDOES signals by sputtering time may be used for finding boundaries of sub-layers of porous PEO coating
- most likely the simplest model of porous PEO coating can be built with three sub-layers
- the first, top sub-layer is the thinnest and most contaminated one and it has a thickness corresponding to sputtering time of about 50 s
- the second, porous sub-layer enriched in phosphorus, oxygen and copper has a thickness corresponding to sputtering time of about 300 s
- the third, transition sub-layer has a thickness corresponding to sputtering time of 550 s
- the porosity boundary from top of the surface down corresponds to the sputtering time of 750 s.

References

[1]   Hryniewicz T, Physico-chemical and technological fundamentals of electropolishing steels (Fizykochemiczne i technologiczne podstawy procesu elektropolerowania stali), 1989, *Monograph* no. 26, Koszalin University of Technology Publishing House; 161 pages.

[2]   Hryniewicz T, On the surface treatment of metallic biomaterials (Wstęp do obróbki powierzchniowej biomateriałów metalowych), 2007, Koszalin University of Technology Publishing House.

[3]   Hryniewicz T, Rokosz K, Zschommler Sandim HR, SEM/EDX and XPS studies of niobium after electropolishing. *Applied Surface Science*, 263 (2012) 357-361.

[4]   Rokicki R, Hryniewicz T, Enhanced oxidation-dissolution theory of electropolishing, *Transactions of The Institute of Metal Finishing,* 90 (2012) 188-196.

[5] Rokosz K, Electrochemical Polishing in magnetic field (Polerowanie elektrochemiczne w polu magnetycznym), 2012, Koszalin University of Technology Publishing House, 211 pages.

[6] Hryniewicz T, Rokicki R, Rokosz K, Co-Cr alloy corrosion behaviour after electropolishing and "magnetoelectropolishing" treatments. *Surface and Coatings Technology*, 62(17-18) (2008) 3073-3076.

[7] Hryniewicz T, Rokosz K, Analysis of XPS results of AISI 316L SS electropolished and magneto-electropolished at varying conditions. *Surface and Coatings Technology*, 204(16-17) (2010) 2583-2592.

[8] Hryniewicz T, Rokicki R, Rokosz K, Magnetoelectropolishing for metal surface modification. *Transactions of The Institute of Metal Finishing*, 85(6) (2007) 325-332.

[9] Hryniewicz T, Rokicki R, Rokosz K, Corrosion and surface characterization of titanium biomaterial after magnetoelectropolishing. *Surface and Coatings Technology*, 203(9) (2008) 1508-1515.

[10] Hryniewicz T, Rokosz K, Polarization characteristics of magnetoelectropolishing stainless steels. *Materials Chemistry and Physics*, 122(1) (2010) 169-174.

[11] Rokosz K, Hryniewicz T, Raaen S, Characterization of passive film formed on AISI 316L stainless steel after magnetoelectropolishing in a broad range of polarization parameters. *Steel Research International*, 83(9) (2012) 910-918.

[12] Hryniewicz T, Rokosz K, Highlights of magnetoelectropolishing, Frontiers in Materials: Corrosion Research, 1(3) (2014) 1-7 (Inaugural Article); DOI: 10.3389/fmats.2014.00003.

[13] Hryniewicz T, Rokosz K, Investigation of selected surface properties of AISI 316L SS after magnetoelectropolishing. *Materials Chemistry and Physics*, 123(1) (2010) 47-55.

[14] Hryniewicz T, Rokosz K, Corrosion resistance of magnetoelectropolished AISI 316L SS biomaterial. *Anti-Corrosion Methods and Materials*, 61(2) (2014) 57-64.

[15] Hryniewicz T, Rokosz K, Valiček J, Rokicki R, Effect of magnetoelectropolishing on nanohardness and Young's modulus of titanium biomaterial. *Materials Letters*, 83 (2012) 69-72.

[16] Hryniewicz T, Rokosz K, Rokicki R, Prima F, Nanoindentation and XPS Studies of Titanium TNZ Alloy after Electrochemical Polishing in a Magnetic Field. *Materials*, 8 (2015) 205-215.

[17] Rokosz K, Hryniewicz T, Simon F, Rzadkiewicz S, Comparative XPS analysis of passive layers composition formed on AISI 304 L SS after standard and high-current density electropolishing. *Surface and Interface Analysis*, 47(1) (2015) 87-92.

[18] Rokosz K, Lahtinen J, Hryniewicz T, Rzadkiewicz S, XPS depth profiling analysis of passive surface layers formed on austenitic AISI 304L and AISI 316L SS after high-current-density electropolishing. *Surface and Coatings Technology*, 276 (2015) 516-520.

[19] Rokosz K, Hryniewicz T, Simon F, Rzadkiewicz S, Comparative XPS analyses of passive layers composition formed on duplex 2205 SS after standard and high-current-density electropolishing. *Tehnicki vjesnik - Technical Gazette*, 23(3) (2016) 731-735.

[20] Rokosz K, Hryniewicz T, Raaen S, Development of Plasma Electrolytic Oxidation for improved Ti6Al4V biomaterial surface properties. *The International Journal of Advanced Manufacturing Technology*, 85 (2016) 2425-2437; DOI: 10.1007/s00170-015-8086-y.

[21] Rokosz K., Hryniewicz T, Raaen S, Chapon P, Investigation of porous coatings obtained on Ti-Nb-Zr-Sn alloy biomaterial by Plasma Electrolytic Oxidation: Characterisation and Modelling. *The International Journal of Advanced Manufacturing Technology*, 2016; DOI 10.1007/s00170-016-8692-3

[22] Rokosz K, Hryniewicz T, Raaen S, Chapon P, Development of copper-enriched porous coatings on ternary Ti-Nb-Zr alloy by Plasma Electrolytic Oxidation. *The International Journal of Advanced Manufacturing Technology*, 2016, DOI 10.1007/s00170-016-9206-z

[23] Rokosz K, Hryniewicz T, Dudek Ł, Matysek D, Valiček J, Harničarova M, SEM and EDS Analysis of Surface Layer Formed on Titanium After Plasma Electrolytic Oxidation in H_3PO_4 with the Addition of $Cu(NO_3)_2$. *Journal of Nanoscience and Nanotechnology*, 16 (2016) 7814-7817.

[24] Rokosz K, Hryniewicz T, Dalibor M, Raaen S, Valiček J, Dudek Ł, Harničarova M, SEM, EDS and XPS Analysis of the Coatings Obtained on Titanium after Plasma Electrolytic Oxidation in Electrolytes Containing Copper Nitrate. *Materials*, 9(318) (2016) 1-12; DOI:10.3390/ma9050318.

[25] Rokosz K, Hryniewicz T, Raaen S, Chapon P, Dudek Ł, GDOES, XPS and SEM with EDS analysis of porous coatings obtained on Titanium after Plasma Electrolytic Oxidation. *Surface and Interface Analysis*, 2016; DOI 10.1002/sia.6136

[26] Gnedenkov SV, Sharkeev YP, Sinebryukhov SL, Khrisanfova OA, Legostaeva EV, Zavidnaya AG, Puz' AV, Khlusov IA, Opra DP, Functional coatings formed on the titanium and magnesium alloys as implant materials by plasma electrolytic oxidation technology: fundamental principles and synthesis conditions. *Corrosion Review*, 34(1-2) (2016) 65-83.

[27] Simka W, Sadowski A, Warczak M, Iwaniak A, Dercz G, Michalska J, Maciej A, Modification of titanium oxide layer by calcium and phosphorus. *Electrochimica Acta*, 56(24) (2011) 8962-8968.

[28] Han Y, Hong SH, Xu KW (2002) Synthesis of nanocrystalline titania films by micro-arc oxidation. *Materials Letters*, 56 (2002) 744-747.

[29] Han Y, Hong SH, Xu KW, Structure and in vitro bioactivity of titania-based films by micro-arc oxidation. *Surface and Coatings Technology*, 168 (2003) 249-258.

[30] Fei C, Hai Z, Chen C, Yangjian X, Study on the tribological performance of ceramic coatings on titanium alloy surfaces obtained through microarc oxidation. *Progress in Organic Coatings*, 64 (2009) 264-267.

[31] Aliasghari S, Plasma Electrolytic Oxidation of Titanium. *PhD Thesis* of Faculty of Engineering and Physical Sciences, The University of Manchester, School of Materials, 2014, 223 pages.

[32] Teh TH, Berkani A, Mato S, Skeldon P, Thompson GE, Habazaki H, Shimizu K (2003) Initial stages of plasma electrolytic oxidation of titanium. *Corrosion Science*, 45 (2003) 2757-2768.

[33] Krząkala A, Mlynski J, Dercz G, Michalska J, Maciej A, Nieuzyla L, Simka W, Modification of Ti-6Al-4V alloy surface by EPD-PEO process in ZrSiO4 suspension. *Archives of Metallurgy and Materials*, 59(1) (2014) 199-204.

[34] Simka W, Nawrat G, Chlode J, Maciej A, Winiarski A, Szade J, Radwanski K, Gazdowicz J, Electropolishing and anodic passivation of Ti6Al7Nb alloy. *Przemysł Chemiczny*, 90(1) (2011) 84-90.

[35] Wang Y, Jiang B, Lei T, Guo L, Dependence of growth features of microarc oxidation coatings of titanium alloy on control modes of alternate pulse. *Materials Letters*, 58 (2004) 1907-1911.

[36] Pulsed RF Glow Discharge Optical Emission Spectrometry - Ultra Fast Elemental Depth Profiling, HORIBA Scientific, Printed in France – ©HORIBA Jobin Yvon: 2014, 7 pages. http://www.horiba.com/scientific/products/atomic-emission-spectroscopy/glow-discharge/ (accessed 29 March 2016).

[37] DiP: Differential Interferometry Profiling. Printed in France – ©HORIBA Jobin Yvon, 2015, 10: 1-4. http://www.horiba.com/fileadmin/uploads/Scientific/Documents/GDS/HJY_BRO_GDO ES_DiP.pdf (accessed on 1 October 2016).